Pharmaceutical Research, Volume 23, No. 2, February 2006 (© 2006)
DOI: 10.1007/s11095-005-9226-0

Research Paper

Expression and Transport Functionality of FcRn within Rat Alveolar Epithelium: A Study in Primary Cell Culture and in the Isolated Perfused Lung

Masahiro Sakagami,[1] Yadollah Omidi,[2,3] Lee Campbell,[2] Lana E. Kandalaft,[2] Christopher J. Morris,[2] Jaleh Barar,[2,3] and Mark Gumbleton[2,4]

Received September 28, 2005; accepted October 21, 2005

Purpose. The neonatal constant region fragment receptor (FcRn) binds and transports IgG. FcRn expression in the upper tracheobronchial airways of the lung is recognized. In this study, we sought to characterize the functional expression of FcRn within alveolar regions of lung tissue.

Methods. FcRn immunohistochemistry was performed on intact rat lung. FcRn expression [Western blot, reverse transcription–polymerase chain reaction (RT-PCR), and immunofluorescence microscopy] and IgG transport functionality were assessed in an *in vitro* rat alveolar epithelial primary cell culture model. An isolated perfused rat lung model was used to examine IgG transport across pulmonary epithelium from airspace to perfusate.

Results. FcRn is expressed in intact alveolar epithelium, substantiated by expression and functionality in an *in vitro* alveolar epithelial model within which IgG transport was temperature sensitive, concentration dependent, and inhibited by excess unlabeled IgG and, to a disproportionate level, by anti-FcRn antibody. Saturable IgG transport across pulmonary epithelium was evident in an isolated perfused rat lung, inhibitable by competing IgG, and displayed a relatively low maximal net IgG absorptive rate of approximately 80 ng/h.

Conclusion. Pulmonary epithelium expresses functional FcRn providing an absorption pathway potentially important for highly potent Fcγ-fusion proteins but unlikely to be of quantitative significance for the systemic delivery of inhaled therapeutic monoclonal IgGs.

KEY WORDS: IgG; isolated perfused lung; lung; neonatal constant region fragment receptor (FcRn); transport.

INTRODUCTION

The neonatal constant region fragment (Fc) receptor (FcRn) is an IgG binding receptor and transporter. FcRn was first identified in the neonatal rodent intestine (1,2), although human fetal intestine also expresses FcRn (3,4). Although species differences exist, FcRn expression has been shown to persist in adulthood in lung epithelial cells of human, mouse, primate (5), and bovine (6) species. FcRn is also expressed within kidney (7), intestine (4), liver (8), lactating mammary gland (9), the syncytiotrophoblast of the placenta (10), and in endothelial cells of the smaller vessels and capillaries (11,12). IgG antibodies bind to FcRn through their Fc domain with high affinity at slightly acidic pH (at or below 6.5) but with negligible binding at or above neutral pH (13,14); IgG subclasses are recognized to display differing affinities for FcRn with IgG1 displaying one of the higher affinity binding interactions in human (15) and rodent (16–18) species. Rodent FcRn seems promiscuous in its binding specificity, able to bind IgG from a wide range of species including human IgGs (hIgGs), whereas human FcRn is more stringent interacting only with IgG from human, rabbit, and guinea pig (17).

Multiple functions for FcRn have been identified in IgG physiology including serving as a rodent neonatal intestinal transporter, mediating placental maternal–fetal transfer, and serving a role in IgG homeostasis through regulating serum IgG half-life via receptor binding and salvaging of IgGs from intracellular lysosomal degradation pathways. Humoral

[1] Department of Pharmaceutics, School of Pharmacy, Virginia Commonwealth University, Richmond, Virginia 23298-0533, USA.
[2] Pharmaceutical Cell Biology, Welsh School of Pharmacy, Cardiff University, Cardiff CF10 3XF, UK.
[3] Present address: Faculty of Pharmacy, Tabriz University of Medical Sciences, Tabriz Iran.
[4] To whom correspondence should be addressed. (e-mail: gumbleton@cardiff.ac.uk)

ABBREVIATIONS: AE, alveolar epithelial; BSA, bovine serum albumin; cDNA, complementary deoxyribonucleic acid; DMEM, Dulbecco's modified Eagle medium; EDTA, ethylenediaminetetraacetic acid; ELISA, enzyme-linked immunosorbent assay; FBS, fetal bovine serum; FcRn, neonatal Fc receptor; FITC, fluorescein isothiocyanate; HRP, horseradish peroxide; IgG, immunoglobulin G; IPRL, isolated perfused rat lung; MDI, metered dose inhaler; MHC, major histocompatibility complex; MWCO, molecular weight cutoff; NIH, National Institute of Health; RT, reverse transcriptase; RT-PCR, reverse transcription–polymerase chain reaction; SDS-PAGE, sodium dodecyl sulfate–polyacrylamide gel electrophoresis; TBST, Tris-buffered saline with Tween 20; tRNA, total RNA; UV, ultraviolet.

defense at mucosal surfaces such as within the lung is an essential element in the body's immune defense. IgGs have been located in the epithelial lining fluid of the lung and observed in bronchoalveolar lavage samples (19,20), with the lung IgG titer present predominantly in the more distal airways (19,21). Recent *in vivo* work (5,22,23) has characterized the spatial expression of FcRn in human, primate, and mouse lung, confirming strong FcRn immunostaining in epithelial cells lining the upper tracheobronchial airways and examining the feasibility of targeting FcRn within this region for the systemic delivery of therapeutic Fcγ -fusion proteins.

In this study, we sought to characterize the spatial expression and functionality of FcRn within the pulmonary regions of rat lung tissue. We used anti-rat FcRn (anti-rFcRn) monoclonal antibody to reveal by immunohistochemistry in rat whole lung tissue the strong immunostaining for FcRn within alveolar epithelium. In primary cultures of rat alveolar epithelium, we confirmed by Western immunoblot, reverse transcription–polymerase chain reaction (RT-PCR), and immunofluorescence microscopy the presence of rFcRn. By flow cytometry, we showed primary cultures of rat alveolar epithelium to uptake labeled rat IgG (rIgG) in a temperature-dependent manner, which could be inhibited with excess unlabeled rIgG and by coincubation with anti-rFcRn antibody. Finally, using an isolated perfused rat lung (IPRL) preparation within which the tracheobronchial circulation is severed, we determined a saturable transport process for airway-administered hIgG across rat pulmonary epithelium.

MATERIALS AND METHODS

Animals

Male-specified pathogen-free Sprague–Dawley rats (Hilltop Lab Animals Inc., Scottsdale, PA, USA, and Charles River Lab Ltd., Margate, Kent, UK) were used throughout and housed in rooms controlled between 20–25°C and 40–70% relative humidity with dark–light cycling every 12 h. The animals had free access to food and water during acclimatization for ≥2 days prior to experimentation. All animal experiments and the protocols described below adhered to the NIH Principles of Laboratory Care USA and the Animal (Scientific Procedures) Act 1986 UK and were approved by Virginia Commonwealth University, USA, and by Cardiff University, UK.

Anti-rFcRn Monoclonal Antibody 1G3

Anti-rFcRn mouse monoclonal antibody 1G3 was generated from an incubation of mouse myeloma hybridoma cells, CRL-2434 (American Type Culture Collection, Manassas, VA, USA), according to the supplier's protocol and published protocol (24). Briefly, cells were plated at a seeding density of 4×10^4 cells/cm^2 in a 25-cm^2 flask, and cultures were maintained in a humidified atmosphere (5% CO_2–95% air) at 37°C with HL-1 medium (BioWhittaker, Walkersville, MD, USA) supplemented with 4 mM L-glutamine (Invitrogen Ltd., Paisley, UK), 1 mM sodium pyruvate (Invitrogen), and 1% fetal bovine serum (FBS; Invitrogen); the medium was replenished every 48 h, and the cells were further cultured to confluency. Collection of 1G3 antibody was over a 48-h period postconfluency with cells cultured in serum-free medium; the harvested media supernatant from this collection period was centrifuged ($100 \times g$ for 10 min) to remove the hybridoma cells. Gel permeation chromatography coupled with ultraviolet (UV) detection (280 nm) had shown this supernatant to yield typically 0.3–0.5 mg of IgG-equivalent molecular weight fraction (≈150 kDa; data not shown). Accordingly, the supernatant was used following optimized dilution in each of the immunohistochemical, immunoblot, and flow cytometric analyses described below.

Immunohistochemical Localization of rFcRn in Intact Rat Alveolar Epithelium

The procedure followed was as described previously (25), except for the use of 1G3 monoclonal antibody. Briefly, lung tissue was fixed by vascular perfusion using highly purified 1% monomeric 0.1 M phosphate-buffered glutaraldehyde (pH 7.4; TAAB Laboratories Equipment Ltd., Berks, UK) for a total of 15 min, after which small specimens of peripheral lung tissue (approximately 1–5 mm^3 in size) were dissected and immersed in the same fixative for a further 2 h. The tissue blocks were then embedded in paraffin wax using a Shanndon (Shanndon, Cheshire, UK) automated tissue processor. Rat lung paraffin wax sections (5–10 μm) were mounted on Superfrost™ microscope slides (Shanndon), the paraffin removed, the sections rehydrated, and endogenous peroxidase activity blocked (0.6% hydrogen peroxide in methanol for 15 min at room temperature). Sections were then briefly washed in tap water before equilibration in Optimax™ wash buffer (pH 7.4; Menerium Diagnostics, Oxford, UK) at room temperature for an additional 10 min. After draining, HL-1 culture supernatant containing 1G3 at dilutions of 1:10, 1:50, and 1:100 was applied to each slide [diluent was 0.6% bovine serum albumin (BSA) in Optimax™ wash buffer] with incubation overnight (15 h) at 4°C within a humidified slide chamber. Dilutions of 1:50 and 1:100 served as serial dilution controls, a further established methodology for verifying specificity. Following this, the sections were further incubated (1 h) with goat anti-mouse secondary antibody conjugated with horseradish peroxidase (HRP–anti-mIgG diluted to 1:100; DakoCytomation Ltd., Cambridgeshire, UK). Subsequently, rFcRn immunostain was generated by 3,3′-diaminobenzidine (DAB) detection (Sigma-Aldrich), with the sections also counterstained with hematoxylin. Parallel sets of sections were used for controls: (1) omission control comprising HL-1 growth media that had not been exposed to 1G3 hybridoma cells in culture and hence lacked 1G3 antibody but nevertheless were subsequently incubated with the secondary HRP–anti-mIgG; (2) isotypic negative control comprising isotypic mouse IgG1 (DakoCytomation) diluted in HL-1 media to equivalent concentrations as the 1G3 antibody with the sections subsequently incubated with the secondary HRP–anti-mIgG. Images were captured using an Olympus BX 41 microscope fitted with a Color View 12 camera and equipped with AnalySIS™ software (Norfolk Analytical Ltd., Norfolk, UK).

Isolation and Culture of Primary Rat AE Cells

Isolation and culture of alveolar epithelial (AE) type II cells were undertaken according to procedures described previously (26). Briefly, rat lung tissue was enzymatically disaggregated using aqueous porcine elastase (2 U/ml; Worthington Biochemical Corporation, Lakewood, NJ, USA). AE type II cells were purified by density centrifugation (250 $\times$ *g* for 20 min) upon a discontinuous Percoll™ gradient (1.040 and 1.089 g/ml; Amersham Biosciences Ltd., Bucks, UK). Following further purification (purity >95%) by differential adherence (1 h), the cells were plated onto tissue culture-treated plastic at a seeding density of 0.9×10^6 cells/cm^2 and cultured at 37°C in 5% CO_2–95% air with Dulbecco's modified Eagle medium (DMEM) supplemented with 10% FBS (Invitrogen), penicillin G (100 U/ml; Invitrogen), gentamicin (50 μg/ml; Invitrogen), and dexamethasone (0.1 μM; Sigma-Aldrich); the medium was replenished every 48 h. The AE type II cells cultured under this protocol have been shown to adopt a phenotype more characteristic of AE type I cells (AE type I-"like") and form a restrictive confluent monolayer (26–30) over the subsequent 6–8 days of culture; in this study, cells were used on day 8 for the Western immunoblot, RT-PCR, and flow cytometric analyses described below.

Western Immunoblot Analysis for rFcRn in Rat AE Cells

Confluent monolayers of AE type-I-"like" cells were harvested on day 8 of culture in lysis buffer as described previously (25). Following centrifugation, the lysate supernatant (equivalent to 30 μg total protein for each sample) was resolved by 15% sodium dodecyl sulfate–polyacrylamide gel electrophoresis (SDS-PAGE) and electroblotted to nitrocellulose membranes (0.2-μm pore size; Schleicher & Schuell, Dassel, Germany); molecular weight markers (Amersham Biosciences) were run concurrently. The membrane was incubated at room temperature for 2 h with 5% nonfat-dried milk in 0.1 M Tris-buffered saline with 0.1% Tween 20 (TBST; pH 7.4), then for 16 h at 4°C with the 1G3-containing culture supernatant (1:10), and finally, for 1 h at room temperature with HRP–anti-mIgG (1:100; DakoCytomation). Chemiluminescence signal was generated using Super Signal Ultra (Pierce, Chester, UK) and recorded onto Hyperfilm ECL (Amersham Biosciences). Soluble truncated rFcRn (~45 kDa) kindly provided by Dr. Björkman (31) was used as positive control.

RT-PCR Analysis for Detecting rFcRn mRNA in Rat AE Cells

Total RNA (tRNA) was harvested from the confluent monolayers of AE type-I-"like" cells on day 8 in TRI reagent (Sigma-Aldrich) using the manufacturer's protocol. The extracted tRNA was quantified using a GeneQuant *pro* RNA/DNA Calculator (Pharmacia Biotech, Cambridge, UK), and 1 μg was subjected to reverse transcription (RT) reaction using 200 U Moloney murine leukemia virus reverse transcriptase (RTase; Invitrogen); this RT recipe was identical to that described previously (25). Samples were denatured at 95°C for 5 min prior to addition of RTase, followed further by incubations at 25°C for 10 min, 42°C for 50 min, 94°C for 5 min, and finally, 4°C for 2 min. The yielded first-strand cDNA was stored at −20°C prior to use.

Aliquots of cDNA were subjected to PCR reaction using custom-made amplification primers 5′-CTGTGGATGAAGCAACCTG-3′ and 5′-TCCACGTTTGACCTCTAGC-3′ (Invitrogen). These were designed against partial mRNA nucleotide sequence of rFcRn (388 bp; GenBank, M35495) using Primer3 program (available at http://frodo.wi.mit.edu/cgi-bin/primer3/primer3_www.cgi). Each PCR reaction was performed in a final volume of 12.5 μl with 2 U *BioTaq* DNA polymerase (Bioline Ltd., London, UK), 0.8 μM each primer, and 2.5 mM $MgCl_2$ using thermal cycler (MJC Research PTC-200; Genetic Research Instrumentation Ltd., Essex, UK). PCR reaction procedures commenced with a denaturation at 95°C for 5 min, followed by amplification with a total of 28 cycles at 95°C for 30 s, 60°C for 45 s, and 72°C for 45 s. A sample from each PCR product was electrophoresed on a 1% agarose gel, and the gel was stained with ethidium bromide for visualization under UV light, as described previously (25). The products were examined with respect to a 1-kbp DNA ladder (Bioline). Negative control samples for RT-PCR reaction omitting either or both cDNA and primers were also prepared and tested. RNA extracted from rat liver homogenate was used as positive tissue control (8). For each RT sample amplified for rFcRn, the housekeeping gene GAPDH was also amplified, and the products were electrophoresed for cross-sample comparison. Conditions for GAPDH RT-PCR were as described previously (25).

Immunofluorescence Microscopy for rFcRn in Rat AE Cells

Primary rat AE type II cells were seeded onto 13-mm glass coverslips and cultured in the presence of dexamethasone for 8 days to achieve a confluent monolayer of AE type-I-"like" cells. On the day of the experiment, cells were washed (×3) with warm phosphate-buffered saline (pH 7.4; PBS) containing 1 mM Ca^{2+} and 1 mM Mg^{2+} (PBS^{++}) and were then fixed for 15 min with 3% paraformaldehyde in PBS at room temperature. After PBS washes, cells were quenched with 50 mM NH_4Cl in PBS for 10 min and were then permeabilized for 5 min with 0.2% Triton X-100 in PBS; for some cell monolayers, this permeabilization step was omitted. Following this, nonspecific binding sites were blocked by a 60-min incubation in blocking buffer (2% v/v FBS, 2% w/v BSA in PBS). Undiluted 1G3-containing culture supernatant from the CRL-2434 hybridoma cell was added to the coverslips for 60 min at room temperature to detect FcRn expression. After washing (3 $\times$ 5 min) with 0.05% v/v Triton X-100 in PBS, cells were then incubated for 30 min with AlexaFluor 488-conjugated chicken anti-mouse secondary antibody (diluted 1:400 in blocking buffer). After washing, cell nuclei were stained with Hoescht and were then mounted and viewed for fluorescence. Fluorescent images were acquired on a Leica DM IRB inverted fluorescent microscope equipped with a 40× oil immersion objective and attached to a Digital CCD Retiga 1300 camera. Images were processed using Adobe Photoshop v7.0 (Adobe Systems, Seattle, WA, USA).

Flow Cytometric Fluorescence Assay for rIgG Uptake into Rat AE Cells

Fluorescein isothiocyanate-conjugated rat IgG (FITC-rIgG; Serotec Ltd., Oxford, UK) was used as a tracer IgG. Following dialysis (MWCO = 2000 Da) overnight at 4°C, various concentrations (0.05–0.4 mg/ml) of FITC-rIgG were prepared in Hank's balanced salt solution supplemented with 10 mM HEPES and 0.15 mM BSA, adjusted at pH 6.5. These solutions were applied to the apical side of confluent (8 days) monolayers of AE type-I-"like" cells grown in 96-well plates, followed by an incubation in the dark for 2 h at either 37 or 4°C. In some wells, 3.0 mg/ml unlabeled rIgG (Serotec) or the 1G3 culture supernatant equivalent to 0.04 mg/ml anti-rFcRn antibody was coincubated with the FITC-rIgG tracer (0.3 mg/ml). Following tracer removal and subsequent acid wash with 0.05 mM citrate–phosphate buffer (pH 5.5; Sigma-Aldrich), the cells were disaggregated with trypsin/ethylenediaminetetraacetic acid (Invitrogen) and pelleted in ice-cold DMEM (pH 7.4). Cell-associated fluorescence distributions (10,000 events per sample) were obtained using flow cytometer (FACSCalibur; Becton Dickinson, Oxford, UK), and the fluorescence of gated cell populations was analyzed using WinMDI (available at http://facs.scrips.edu/software.html). Median fluorescence intensity of each fluorescence population was used to evaluate FITC-rIgG uptake into these cells.

Pulmonary Transport (Airway to Perfusate) of hIgG in the IPRL

The IPRL preparation and the forced solution instillation were developed and validated in-house and used unchanged, as described in detail previously (32,33). Briefly, a rat lung was surgically removed and housed horizontally in an artificial thorax maintained at 37°C. Krebs–Henseleit buffer containing 4% (w/v) BSA was used as perfusate and recirculated through the pulmonary circulation at a constant flow rate of 15 ml/min. To differentiate absorbed antibody from endogenous counterpart appearing into perfusate, hIgG (EMD Biosciences, Inc., San Diego, CA, USA) was used as the tracer IgG by virtue of its ability to bind rFcRn with similar affinity to rIgG (14). hIgG solutions were prepared with 0.05 M PBS (pH 6.5) at 0.3 or 2.5 mg/ml with or without competing aliquot of 3.0 mg/ml rIgG (Serotec). Each of these solutions (0.1 ml) was administered into the airways of the IPRL as a coarse spray by a single actuation of a propellant-only metered dose inhaler, thereby completing the forced solution instillation (32). This inflates the lung with about 5.5 ml of propellant vapor and simultaneously accomplishes the "forced solution instillation." Perfusate samples (0.5 ml) were withdrawn from the reservoir at different time intervals following instillation, and volumes were replaced with fresh perfusate immediately after sampling. The hIgG concentration in these samples was determined in triplicate by enzyme-linked immunosorbent assay for hIgG (Bethyl Laboratories, Inc., Montgomery, TX, USA) that was only slightly modified from the manufacturer's protocol to improve the lower limit of quantification, specifically changing the dilution factor for secondary antibody (1:20,000) and the enzyme substrate reaction period (45 min); the effect of these changes on assay accuracy and precision was assessed in-house. Indeed, the assay showed negligible cross-reactivity with rIgG and was validated with acceptable assay precision (% relative standard deviation $\leq 18.5\%$) and accuracy (% error $\leq 13.2\%$) for perfusate samples in the range of 0.1–2.0 ng/ml. The kinetics of hIgG absorption from the IPRL was characterized by its appearance in perfusate (concentration multiplied by perfusate volume) over time. The IPRL was found to be viable for $\geq$120 min, as evidenced by the absence of pulmonary edema (33) and/or any notable discontinuity in hIgG airway-to-perfusate transfer *vs.* time profiles.

Statistics

Results are presented as mean ± SD unless otherwise stated. Statistical analysis was undertaken using analysis of variance with *post hoc* analysis by Duncan's multiple range test and Student–Newman–Keuls (flow cytometry) or non-paired Student's *t* test (IPRL). Details are provided in the figure legends. Statistical significance was at $p < 0.05$ unless otherwise stated.

RESULTS

Immunohistochemical Localization of rFcRn in Intact Rat Alveolar Epithelium

Paraffin wax sections (5–10 μm) of rat normal lung tissue were prepared and immunostained for FcRn using the secreted anti-FcRn monoclonal antibody harvested in serum-free growth media collected over a 48-h period from 1G3 hybridoma cell cultures. Shown in Fig. 1 is the immunohistochemical staining for rFcRn in the rat lung tissue. Using the 1G3 monoclonal anti-rFcRn (1:10 dilution), bronchial epithelium is clearly labeled positive for DAB immunostain (Fig. 1A). To varying degrees, rFcRn expression seemed evident also in vascular endothelium as well as smaller arterioles and venules, whereas perivascular lymphatics, mesothelium, pleura, and other supporting tissues seemed devoid of immunostain (not shown). Figure 1B shows an isotypic (IgG1) negative control image (antibody concentration equivalent to that of the 1:10 1G3 antibody dilution) of a bronchial epithelium devoid of any DAB (brown) immunostain. Omission controls showed a similar negative appearance (data not shown). Furthermore, serial dilution controls for 1G3 antibody through to 1:50 and 1:100 resulted in progressively reduced intensity of staining. Significantly, immunolabeling with 1G3 (1:10) showed marked immunostaining for rFcRn across the entire AE surface (Fig. 1C), with the alveolar sections treated with isotypic control (Fig. 1D) and omission control lacking any indicative staining. Figure 1E shows a higher magnification image of rFcRn immunostaining of the alveolar airspace highlighting luminal surface staining of the pulmonary epithelial–endothelial barrier.

Western Immunoblot Analysis for rFcRn in Rat AE Cells

Figure 2 is a Western immunoblot for rFcRn detected using 1G3 culture supernatant in lysates from primary

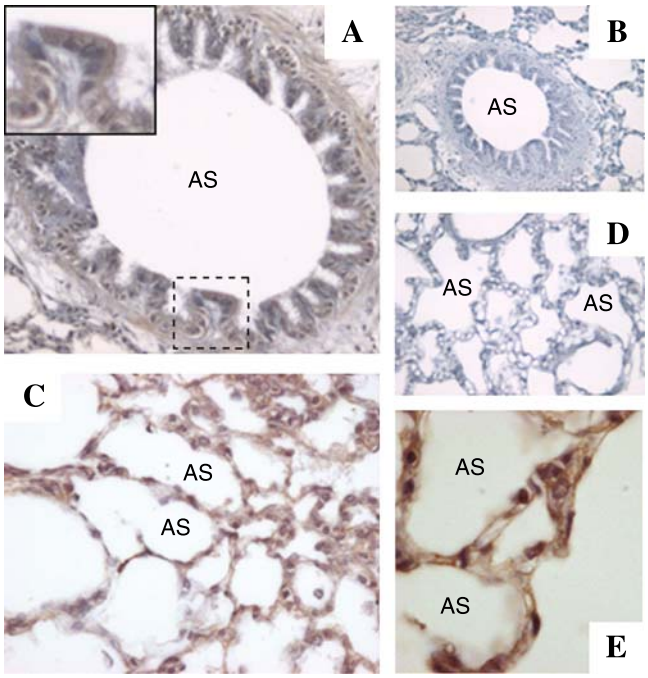

Fig. 1. Immunohistochemical staining for rat FcRn (rFcRn) in paraffin sections (5- to 10-μm thickness) of rat normal lung tissue. (A) Bronchial epithelium reveals immunostaining with 1G3 monoclonal anti-rFcRn (1:10 dilution). The insert highlights a bronchial fold within which immunostained bronchial epithelial cells are clearly seen. (B) Isotypic (IgG1) negative control image (antibody concentration equivalent to that of the 1:10 1G3 antibody dilution) of a bronchial epithelium devoid of immunostain. Omission controls (not shown) displayed a similar negative appearance. (C) Anti-rat FcRn (1:10 dilution) immunostaining across the entire alveolar epithelial surface, with alveolar sections exposed to isotypic control (D) and omission control (not shown) lacking staining. (E) Higher magnification (×60) image of rFcRn immunostaining of the alveolar airspace. Sections were prepared from three separate animals with the sections shown representing consensus staining profiles. Magnification: B, D ×20; A, C ×30. AS = airspace.

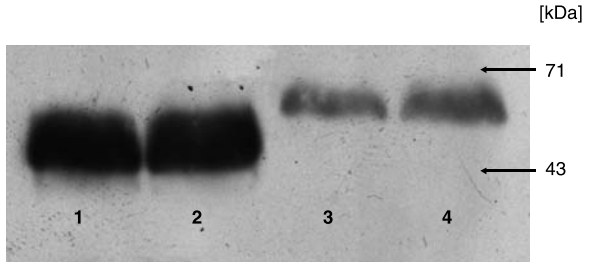

Fig. 2. Representative Western immunoblot showing expression of rFcRn in rat alveolar epithelial (AE) type-I-"like" cells harvested on day 8 of primary culture. Lanes 1 and 2: soluble truncated rFcRn protein (~45 kDa) used as positive control [31]; lanes 3 and 4: cell lysates harvested from rat AE type-I-"like" cells and showing signal for the nontruncated form of rFcRn. Analysis replicated three times with separate primary cultures. Molecular weights were determined relative to based concurrently run rainbow molecular weight marker.

cultures of rat AE type-I-"like" cells grown to day-8 postseeding. Soluble truncated rFcRn was used as a positive control (31) and generated a clear band signal migrating appropriately to ~45 kDa (lanes 1 and 2 in Fig. 2). Expression of rFcRn was substantiated in the cultured AE type-I-"like" cells (day 8) by specific band signals that, as expected for the nontruncated form, migrated to a molecular weight of ~50–60 kDa (lanes 3 and 4 in Fig. 2); the difference in migration may, in addition to truncation, be also caused by differences in glycosylation between the nontruncated and truncated forms as suggested for this protein by others (31).

RT-PCR Analysis for Detecting rFcRn mRNA in Rat AE Cells

Figure 3 shows representative agarose gels of the amplified gene products for rFcRn mRNA (top) and the housekeeper gene GAPDH (bottom) from the cultured rat day-8 AE type-I-"like" cells grown in the absence (lanes 5–7) or presence (lanes 8–10) of dexamethasone 0.1 μM. Control lanes comprised, as a positive check, rat liver homogenate (lane 4) alongside respective negative controls for rFcRn (lanes 1–3), where in lanes 1 and 2, template cDNA is missing and strong primer–dimer formation is evident, and in lane 3, the PCR primers themselves are omitted. Whereas negative controls showed no signals other than primer–dimers, both the AE type-I-"like" cell samples (lanes 5–10) and the liver homogenate sample (line 4) gave clear bands at ~390 bp consistent with the predicted amplified rFcRn product size (i.e., 388 bp) generated from use of these particular designed primers. The growth of the rat AE cells in media containing 0.1 μM dexamethasone seemed not to affect, at least in a semiquantitative manner, rFcRn transcript levels (lanes 5–7 *vs.* lanes 8–10) in the cells (note that the GAPDH signal was consistent between the treatments).

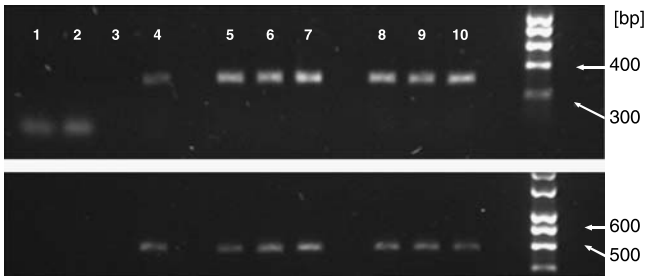

Fig. 3. Agarose gel of the RT-PCR analysis for rFcRn (top) and the housekeeper gene GAPDH (bottom) from total RNA harvested from rat AE type-I-"like" cells on day 8 of primary culture. Lane 1: Room temperature control with primers; lane 2: no cDNA with primers; lane 3: rat liver cDNA without primers; lane 4: as positive control rat liver cDNA with primers; lanes 5–7 cDNA from rat AE type-I-"like" cells grown in the absence (lanes 5–7) or presence (lanes 8–10) of dexamethasone 0.1 μM. Whereas negative controls showed no signals other than primer–dimers, both the AE type-I-"like" cell samples (lanes 5–10) and the liver homogenate sample (line 4) gave clear bands at ~390 bp consistent with the predicted amplified rFcRn product size (i.e., 388 bp). GAPDH signal appears consistent between the alveolar cells grown in the absence or presence of dexamethasone. Analysis replicated three times with separate primary cultures.

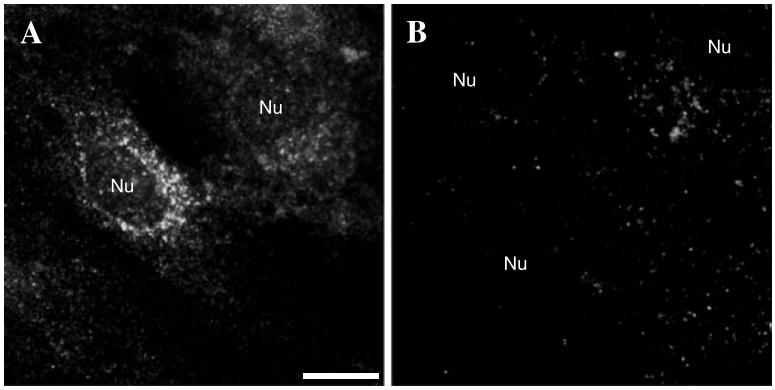

Fig. 4. Primary rat alveolar epithelial type-I-"like" cells cultured in the presence of dexamethasone for 8 days and immunostained for rFcRn using 1G3 monoclonal antibody with AlexaFluor 488-conjugated chicken anti-mouse secondary antibody. (A) In cells permeabilized prior to immunostaining with 0.2% Triton X-100 for 5 min, an immune-specific punctate labeling for FcRn throughout the body of each cell was observed. (B) In cells where permeabilization was omitted, only a slight immunostain was evident with the appearance of localization to the cell surface. Scales bar: 10 μm. Nu: a cell nucleus. Analysis replicated three times with separate primary cultures.

Immunofluorescence Microscopy for FcRn within Rat AE Cells

Immunofluorescence microscopy was undertaken to examine for FcRn expression in the rat alveolar type-I-"like"cells (Fig. 4). In cells permeabilized with 0.2% Triton X-100, to afford access of the anti-rFcRn antibody (1G3) to intracellular targets, an immune-specific punctate labeling for FcRn throughout the body of each cell was observed (Fig. 4A). In contrast, in cells where permeabilization was omitted and, as a consequence, antibody access to intracellular targets was excluded, only a slight immunostain was evident with the appearance of localization to the cell surfaces (Fig. 4B). A similar distribution pattern was evident in cells initially incubated at pH 6.5 (data not shown). These data indicate that the majority of FcRn in the cultured alveolar cell phenotype is intracellularly located.

Flow Cytometric Fluorescence Assay for rIgG Uptake into Rat AE Cells

Figure 5 shows the results of flow cytometric examination of rIgG cell association with the rat AE type-I-"like" primary cultured cells. The aqueous media used for the studies was buffered to pH 6.5, a pH that affords high-affinity binding of IgG Fc domains to FcRn. Incubations of FITC-rIgG at 37°C shifted cell-associated fluorescence distributions toward a higher fluorescent intensity (e.g., Fig. 5A), indicative of cell association (cell uptake and/or binding) of FITC-rIgG by the AE type-I-"like" cells. This cell association seemed to increase with increases in the concentration of FITC-rIgG, at least up to 0.4 mg/ml (Fig. 5B; all groups significantly different at $p < 0.05$ from each other), although there was a clear evidence that the cell association over this concentration range was subject to a saturable phenomenon as an 8-fold increase in apical FITC-rIgG concentration

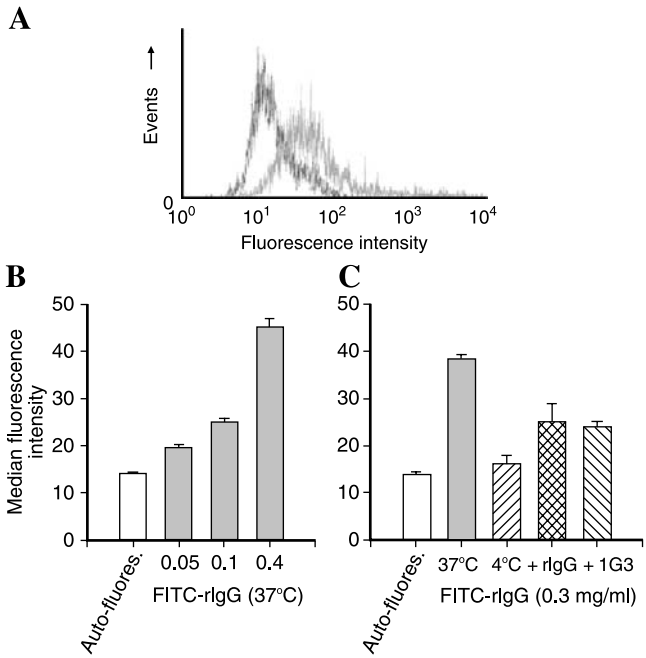

Fig. 5. Flow cytometric fluorescence assay for rIgG uptake into primary cultures of rat AE type-I-"like" cells. (A) Typical cell-associated fluorescence distribution (10,000 events per sample) shift within AE type-I-"like" cells incubated with buffer (pH 6.5) and fluorescein isothiocyanate-conjugated rat IgG (FITC-rIgG, 0.3 mg/ml) for 2 h at 37°C. (B) Median fluorescence intensity following 2 h 37°C incubation of buffer (pH 6.5) "autofluorescence" and FITC-rIgG at 0.05, 0.1, and 0.4 mg/ml. (C) Median fluorescence intensity following 2-h incubation of buffer (pH 6.5) and FITC-rIgG (0.3 mg/ml) at either 37 or 4°C, in the absence or presence of 3.0 mg/ml unlabeled rIgG or of 0.04 mg/ml anti-rFcRn antibody (1G3). Cell association was suppressed ($p < 0.05$) almost completely at 4°C and competitively inhibited (50%) by a 10-fold excess of unlabeled rIgG and by low concentrations of anti-rFcRn antibody. Histogram data (B, C) represent mean ± standard deviation from $n = 3$. Analysis replicated twice with separate primary cultures.

resulted in only an approximately 4-fold increase in cell association (when autofluorescence is accounted for). The cell association was suppressed ($p < 0.05$) almost completely at 4°C (Fig. 5C), suggesting the involvement of an energy-dependent uptake process. Furthermore, competitive incubation with unlabeled rIgG (3.0 mg/ml), a 10-fold excess concentration compared to FITC-rIgG tracer, caused an approximately 50% inhibition in FITC-rIgG cell association (Fig. 5C; $p < 0.05$) compared to 37°C control. Coincubation with anti-rFcRn antibody (1G3 culture supernatant at an antibody concentration of approximately 0.04 mg/ml), at a concentration of only 13% of the FITC-rIgG tracer concentration, also caused an approximately 50%% inhibition ($p < 0.05$) in FITC-rIgG cell association (Fig. 5C) compared to 37°C control. Collectively, these results demonstrate a temperature-dependent cell association of FITC-rIgG with the rat AE type-I-"like" primary cultured cells, an association that, at least in part, involves a specific cell uptake process and one mediated via the FcRn receptor.

Pulmonary Absorption of hIgG in the IPRL

Figure 6 shows the cumulative mass of hIgG transferred from the airways of the IPRL into the perfusate following a 0.1-ml forced solution (pH 6.5) instillation of 0.3 and 2.5 mg/ml of hIgG (nominal doses of 0.03 and 0.25 mg, respectively). Also shown in Fig. 6 is the cumulative profile of a 0.3-mg/ml hIgG instillation coadministered with 3.0 mg/ml rIgG (pH 6.5). Transport of hIgG from the 0.3- and 2.5-mg/ml solutions appeared linear over the 2-h experimental period with respective transport rates of 73.6 ± 18.5 and 85.6 ± 22.9 ng/h (mean ± SD, $n = 4$; $p > 0.05$ by unpaired Student's t test). This apparent lack of dose proportionality suggested the operation of a saturable transport system for hIgG within this IPRL. When hIgG (0.3-mg/ml solution; dose 0.03 mg) was coadministered with a 10-fold excess of rIgG, the transport of hIgG was significantly suppressed to a rate of 28.2 ± 10.8 ng/h ($p < 0.05$ *vs.* the respective 0.3-mg/ml hIgG instillation in the absence of coadministered rIgG), indicative of a competitive transport process between the IgG molecules, possibly via rFcRn. This observation of competition between hIgG and rIgG is to be expected if the mechanism involves FcRn transport, as IgG molecules from human and rat species display similar affinity for rFcRn (14).

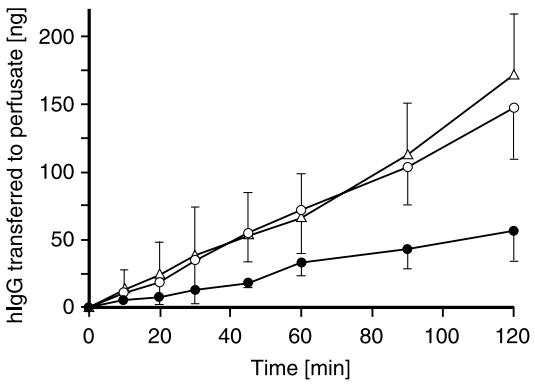

Fig. 6. Cumulative mass of human IgG (hIgG) transferred from the airways of the IPRL into the perfusate following a 0.1 ml forced solution (pH 6.5) instillation of 0.3 and 2.5 mg/ml of hIgG (nominal doses of 0.03 and 0.25 mg, respectively). When hIgG (0.3-mg/ml solution; dose 0.03 mg) coadministered with a 10-fold excess of rIgG, the transport of hIgG was significantly ($p < 0.05$) suppressed compared to the respective 0.3-mg/ml hIgG instillation in the absence of coadministered rIgG. Data represent mean ± standard deviation from $n = 4$. Dosing solution: (○) 0.3 mg/ml hIgG; (△) 2.5 mg/ml hIgG; (●) 0.3 mg/ml hIgG + 3.0 mg/ml rat IgG (rIgG).

DISCUSSION

We sought to examine the expression and functionality of FcRn within alveolar epithelium of normal adult rat lung. Using a monoclonal antibody specific for rFcRn (31), our immunohistochemical analysis showed FcRn immunostain localized to bronchial epithelial cells and as an uninterrupted layering across the alveolar airspace surfaces, with then intensity of immunostaining between these two zones comparable. Spiekermann *et al.* (5), using a polyclonal antibody against a conserved peptide domain within rFcRn, assessed FcRn expression within human and macaque adult lung and found FcRn within bronchial epithelial cells lining the large and small airways but, in alveolar tissue, reported only weak immunostain that appeared in a randomly scattered pattern that they hypothesized as may be a result of alveolar macrophages. We interpret that the FcRn staining in our current work within the alveolar region of rat lung tissue does not arise from a technical anomaly, although we cannot completely exclude, however unlikely, that the continuous pattern of alveolar FcRn immunostain arises from a heavy and uniform contamination of alveolar macrophages, albeit pathogen-free animals were used in experiments. Species differences may exist in the spatial pattern of FcRn expression within lung tissue, or the primary FcRn antibodies used for immunohistochemistry in the various laboratories may differ in their capacity to reveal low-density epitopes in what is at best only a semi-quantitative methodology.

The alveolar type II epithelial cell serves as the *in vivo* progenitor for, and differentiates into, the alveolar type I epithelial cell that occupies approximately 95% of the AE surface area. A similar process is documented to occur *in vitro* during a 5- to 8-day primary culture of rat type II cells leading to a type-I-"like" phenotype (26,29,30). Rat alveolar type II cells are isolated to a purity of greater than 90% (26), and following 48 h in culture with media changes, any contaminating cells, if present, will comprise less than 1–2% of the population. Within these highly pure primary cultures, we confirmed the presence of FcRn mRNA and protein expression within this cultured type-I-like AE cell at day-8 postseeding and noted by immunofluorescence microscopy that the majority of the FcRn immunostain appeared intracellular. Using a similar primary culture model, Kim *et al.* (34) have recently reported the presence of rFcRn mRNA transcript in day-6 cultures. These results provide a consensus and support our interpretation that FcRn immunostaining within the rat alveolar lung sections reflects localization predominantly to the epithelium.

Dexamethasone is often included in the media for primary rat AE culture to aid the generation of a restrictive paracellular barrier (27). Our own results show FcRn mRNA levels within the primary AE cultures to remain unaffected

by the presence, throughout the 8-day culture period, of dexamethasone (0.1 μM). This is contradictory to the results of Kim *et al.* (34) who showed that days 3–6 primary AE cultures exposed for 72 h to 0.1 μM dexamethasone displayed a reduced FcRn RNA signal. Such divergent observations may well reflect differences in culture media and conditions. No other reports of the effects of glucocorticoid upon FcRn expression have been made, although glucocorticoids have been shown to lead to a loss of Fcγ receptor expression in intestinal enterocytes of newborn suckling rats (35) or reductions *in vitro* of both basal and IFNγ-induced expressions of FcγRI in leucocyte cell lines, although such effects seem to be cell specific (36) and indeed Fc receptor subtype specific (37).

Using flow cytometry, we undertook IgG uptake studies upon AE type-I-"like" cell monolayers with the apical media buffered to pH 6.5 favoring IgG–FcRn interactions at the cell surface; the use of pH 6.5 is consistent with lung lining fluid reported to possess a slightly acidic pH (38,39). Our *in vitro* studies conducted at apical concentrations of FITC-rIgG between 0.05 and 0.4 mg/ml (0.33–2.7 μM) revealed an uptake route that showed some evidence of concentration dependency with indications of an affinity in the low micromolar to high nanomolar range, and one that was temperature sensitive and competitively inhibited by unlabeled rIgG, and reduced to a disproportionately greater extent by anti-rFcRn antibody. The interaction of IgG with immobilized FcRn is acknowledged to involve two independent binding interactions (18). Studies of IgG interaction with immobilized rFcRn report affinity constants of approximately 34 nM (rat IgG1) for the high-affinity slow-dissociating binding interaction and affinity constants of approximately 1 μM for the low-affinity fast-dissociating binding interaction (18). Depending on the particular rIgG isotype involved, similar values of between 0.15 and 1 μM have been reported by others (16,40) for the low-affinity binding interaction. Clearly, the IgG concentrations used in our uptake studies (between 0.33 and 2.7 μM) would saturate the high-affinity binding interactions, and any evidence of a concentration dependency in our data would be reflective of the increasing occupation of the low-affinity interaction sites. In the *in vitro* transcellular AE studies of Kim *et al.* (34), conducted at pH 7.4, a saturable process for IgG transport was revealed of high affinity (IgG concentrations at half-maximal flux estimated at 16 nM for the apical to basal transport) and low capacity (respective maximal flux of 2.0 fmol cm^{-2} h^{-1}); despite IgG concentrations up to 25 μM, their data did not, however, reveal the presence of a lower-affinity IgG–FcRn binding interaction. Furthermore, IgG transport in their transcellular model seemed not to be affected by incremental decreases in apical chamber pH from 7.4 to 5.5, implying that binding of IgG by FcRn receptor at the cell surface did not, in its own right, trigger membrane internalization. As a corollary, this would imply internalization occurring at the same rate regardless of whether capture at the plasma membrane is by receptor-mediated endocytosis (extracellular fluid at acidic conditions) or fluid phase endocytosis (extracellular fluid at neutral or slightly alkaline conditions).

To further examine IgG transport within the distal air spaces in a model that maintained an intact pulmonary lung architecture, but without the complicating issues of whole animal systemic pharmacokinetics, we undertook IPRL studies. The concentrations of hIgG instilled as a forced solution (pH 6.5) were 2 and 17 μM, both of which would saturate FcRn high-affinity binding interactions, and with the lower administered concentration (2 μM) approximating the reported affinity constant for the low-affinity binding interaction. Consistent with a saturable absorption pathway for hIgG transport from the distal lung to pulmonary perfusate, we observed essentially similar transport rates between these two (8.5-fold different) concentrations. The involvement of a receptor-mediated process was further confirmed by the competitive inhibition in transport of the 2-μM hIgG forced instillate by coadministered rIgG. The bronchial circulation is severed in isolated perfused lung preparations, although the pulmonary circulation is maintained. As such, the absorption we observe is reflective of transport across pulmonary epithelium. Our data provide a maximal IgG absorption rate of ~80 ng/h (corresponding to ~536 fmol h^{-1}), which, for the AE surface area of a 0.3-kg rat (~2.8 m^2—estimated by allometric scaling), would equate to a flux of ~0.02 fmol cm^{-2} h^{-1}. This flux is 100-fold smaller than the maximal flux (2 fmol cm^{-2} h^{-1}) determined across cultured *in vitro* alveolar epithelium by Kim *et al.* However, it is reasonable to assume that only a small proportion of the forced instillate (10%) will have reached the pulmonary absorption surfaces and indeed that not all alveoli will be accessible to the dose. Nevertheless, these data reemphasize the relatively low rate of IgG transport across the pulmonary epithelial barrier, an absorption rate if allometrically scaled to a 70-kg human would equate to ~3 μg/h. Such an absorption rate would not readily afford achievement of target serum concentrations of 0.5–1 μg/ml that are most commonly observed for systemically acting therapeutic antibodies. The accomplishments of Syntonix Pharmaceuticals and collaborating laboratories (5,22,23) exploiting FcRn in the lung for the absorption of systemically acting chimeric Fcγ-fusion proteins almost certainly benefit from their selection within the chimeric molecule of highly potent peptide or protein therapeutics, such as erythropoietin and follicle-stimulating hormone. These are active at much lower concentrations than therapeutic monoclonal antibodies.

In summary, using a variety of techniques and tissue models from *in vitro* cell culture to the intact *ex vivo* lung, we have characterized the spatial and functional expression of FcRn within the pulmonary alveolar tissues of rat lung. Pulmonary epithelial FcRn is unlikely to be of quantitative significance for the systemic delivery of inhaled therapeutic monoclonal IgGs, although potentially important for highly potent Fcγ-fusion proteins. This work will be noteworthy for investigations examining pulmonary IgG homeostatic physiology and in pharmaceutical studies seeking to exploit the FcRn receptor for the absorption of Fcγ-based macromolecule therapeutics.

ACKNOWLEDGMENTS

The authors are grateful to Pamela J. Björkman, Ph.D., Division of Biology, California Institute of Technology, Pasadena, CA, USA, for her gift of truncated rFcRn. This research began during MS's 2-month research leave at

Cardiff University (CU) and was supported in part by the Medical College of Virginia Foundation, Richmond, VA, USA, and by MG's research funds at Cardiff University, UK. MS and MG acknowledge the encouragement of Peter Byron, Ph.D., School of Pharmacy Virginia Commonwealth University, throughout this work.

REFERENCES

1. R. Rodewald and J. P. Kraehenbuhl. Receptor-mediated transport of IgG. *J. Cell Biol.* **99**:159–164 (1984).
2. N. E. Simister and A. R. Rees. Isolation and characterisation of an Fc receptor from neonatal rat small intestine. *Eur. J. Immunol.* **15**:733–738 (1985).
3. U. Shah, B. L. Dickinson, R. S. Blumberg, N. E. Simister, W. I. Lencer, and W. A. Walker. Distribution of the IgG Fc receptor, FcRn, in the human fetal intestine. *Pediatr. Res.* **53**:295–301 (2003).
4. E. J. Israel, S. Taylor, Z. Wu, E. Mizoguchi, R. S. Blumberg, A. Bhan, and N. E. Simister. Expression of the neonatal Fc receptor, FcRn, on human intestinal epithelial cells. *Immunology* **92**:69–74 (1997).
5. G. M. Spiekermann, P. W. Finn, E. S. Ward, J. Dumont, B. L. Dickinson, R. S. Blumberg, and W. I. Lencer. Receptor-mediated immunoglobulin G transport across mucosal barriers in adult life: functional expression of FcRn in the mammalian lung. *J. Exp. Med.* **196**:303–310 (2002).
6. B. Mayer, Z. Kis, G. Kajan, L. V. Frenyo, L. Hammarstrom, and I. Kacskovics. The neonatal Fc receptor (FcRn) is expressed in the bovine lung. *Vet. Immunol. Immunopathol.* **98**:85–89 (2004).
7. J. P. Haymann, J. P. Levraud, S. Bouet, V. Kappes, J. Hagege, G. Nguyen, Y. Xu, E. Rondeau, and J. D. Sraer. Characterization and localization of the neonatal Fc receptor in adult human kidney. *J. Am. Soc. Nephrol.* **11**:632–639 (2000).
8. R. S. Blumberg, T. Koss, C. M. Story, D. Barisani, J. Polischuk, A. Lipin, L. Pablo, R. Green, and N. E. Simister. A major histocompatibility complex class I-related Fc receptor for IgG on rat hepatocytes. *J. Clin. Invest.* **95**:2397–2402 (1995).
9. P. Cianga, C. Cianga, L. Cozma, E. S. Ward, and E. Carasevici. The MHC class I related Fc receptor, FcRn, is expressed in the epithelial cells of the human mammary gland. *Hum. Immunol.* **64**:1152–1159 (2003).
10. N. E. Simister. Placental transport of immunoglobulin G. *Vaccine* **21**:3365–3369 (2003).
11. J. Borvak, J. Richardson, C. Medesan, F. Antohe, C. Radu, M. Simionescu, V. Ghetie, and E. S. Ward. Functional expression of the MHC class I-related receptor, FcRn, in endothelial cells of mice. *Int. Immunol.* **10**:1289–1298 (1998).
12. F. Schlachetzki, C. Zhu, and W. M. Pardridge. Expression of the neonatal Fc receptor (FcRn) at the blood–brain barrier. *J. Neurochem.* **81**:203–206 (2002).
13. M. Raghavan, L. N. Gastinel, and P. J. Bjorkman. The class I major histocompatibility complex related Fc receptor shows pH-dependent stability differences correlating with immunoglobulin binding and release. *Biochemistry* **32**:8654–8660 (1993).
14. M. Raghavan, V. R. Bonagura, S. L. Morrison, and P. J. Bjorkman. Analysis of the pH dependence of the neonatal Fc receptor/immunoglobulin G interaction using antibody and receptor variants. *Biochemistry* **34**:14649–14657 (1995).
15. A. P. West Jr. and P. J. Bjorkman. Crystal structure and immunoglobulin G binding properties of the human major histocompatibility complex-related Fc receptor(,). *Biochemistry* **39**:9698–9708 (2000).
16. C. Medesan, P. Cianga, M. Mummert, D. Stanescu, V. Ghetie, and E. S. Ward. Comparative studies of rat IgG to further delineate the Fc:FcRn interaction site. *Eur. J. Immunol.* **28**:2092–2100 (1998).
17. R. J. Ober, C. G. Radu, V. Ghetie, and E. S. Ward. Differences in promiscuity for antibody–FcRn interactions across species: implications for therapeutic antibodies. *Int. Immunol.* **13**:1551–1559 (2001).
18. D. E. Vaughn and P. J. Bjorkman. High-affinity binding of the neonatal Fc receptor to its IgG ligand requires receptor immobilization. *Biochemistry* **36**:9374–9380 (1997).
19. W. W. Merrill, G. P. Naegel, J. J. Olchowski, and H. Y. Reynolds. Immunoglobulin G subclass proteins in serum and lavage fluid of normal subjects: quantitation and comparison with immunoglobulins A and E. *Am. Rev. Respir. Dis.* **131**:584–587 (1985).
20. H. Y. Reynolds and H. Newball. Analysis of proteins and respiratory cells obtained from human lungs by bronchial lavage. *J. Lab. Clin. Med.* **84**:559–573 (1974).
21. R. Kitz, P. Ahrens, and S. Zielen. Immunoglobulin levels in bronchoalveolar lavage fluid of children with chronic chest disease. *Pediatr. Pulmonol.* **29**:443–451 (2000).
22. A. J. Bitonti, J. A. Dumont, S. C. Low, R. T. Peters, K. E. Kropp, V. J. Palombella, J. M. Stattel, Y. Lu, C. A. Tan, J. J. Song, A. M. Garcia, N. E. Simister, G. M. Spiekermann, W. I. Lencer, and R. S. Blumberg. Pulmonary delivery of an erythropoietin Fc fusion protein in non-human primates through an immunoglobulin transport pathway. *Proc. Natl. Acad. Sci. USA* **101**:9763–9768 (2004).
23. S. C. Low, S. L. Nunes, A. J. Bitonti, and J. A. Dumont. Oral and pulmonary delivery of FSH-Fc fusion proteins via neonatal Fc receptor-mediated transcytosis. *Hum. Reprod.* **20**:1805–1813 (2005).
24. M. Raghavan, M. Y. Chen, L. N. Gastinel, and P. J. Bjorkman. Investigation of the interaction between the class I MHC-related Fc receptor and its immunoglobulin G ligand. *Immunity* **1**:303–315 (1994).
25. L. Campbell, A. N. Abulrob, L. E. Kandalaft, S. Plummer, A. J. Hollins, A. Gibbs, and M. Gumbleton. Constitutive expression of P-glycoprotein in normal lung alveolar epithelium and functionality in primary alveolar epithelial cultures. *J. Pharmacol. Exp. Ther.* **304**:441–452 (2003).
26. L. Campbell, A. J. Hollins, A. Al-Eid, G. R. Newman, R. C. von, and M. Gumbleton. Caveolin-1 expression and caveolae biogenesis during cell transdifferentiation in lung alveolar epithelial primary cultures. *Biochem. Biophys. Res. Commun.* **262**:744–751 (1999).
27. J. M. Cheek, K. J. Kim, and E. D. Crandall. Tight monolayers of rat alveolar epithelial cells: bioelectric properties and active sodium transport. *Am. J. Physiol.* **256**:C688–C693 (1989).
28. J. M. Cheek, M. J. Evans, and E. D. Crandall. Type I cell-like morphology in tight alveolar epithelial monolayers. *Exp. Cell Res.* **184**:375–387 (1989).
29. S. I. Danto, S. M. Zabski, and E. D. Crandall. Reactivity of alveolar epithelial cells in primary culture with type I cell monoclonal antibodies. *Am. J. Respir. Cell Mol. Biol.* **6**:296–306 (1992).
30. L. G. Dobbs, M. C. Williams, and R. Gonzalez. Monoclonal antibodies specific to apical surfaces of rat alveolar type I cells bind to surfaces of cultured, but not freshly isolated, type II cells. *Biochim. Biophys. Acta* **970**:146–156 (1988).
31. L. N. Gastinel, N. E. Simister, and P. J. Bjorkman. Expression and crystallization of a soluble and functional form of an Fc receptor related to class I histocompatibility molecules. *Proc. Natl. Acad. Sci. USA* **89**:638–642 (1992).
32. P. R. Byron and R. W. Niven. A novel dosing method for drug administration to the airways of the isolated perfused rat lung. *J. Pharm. Sci.* **77**:693–695 (1988).
33. M. Sakagami, P. R. Byron, J. Venitz, and F. Rypacek. Solute disposition in the rat lung *in vivo* and *in vitro*: determining regional absorption kinetics in the presence of mucociliary escalator. *J. Pharm. Sci.* **91**:594–604 (2002).
34. K. J. Kim, T. E. Fandy, V. H. Lee, D. K. Ann, Z. Borok, and E. D. Crandall. Net absorption of IgG via FcRn-mediated transcytosis across rat alveolar epithelial cell monolayers. *Am. J. Physiol., Lung Cell Mol. Physiol.* **287**:L616–L622 (2004).
35. P. Griffin and A. E. Wild. Effect of dexamethasone on Fc gamma receptor expression in foetal and neonatal rat gut. *Experientia* **44**:242–245 (1988).
36. L. Y. Pan, D. B. Mendel, J. Zurlo, and P. M. Guyre. Regulation of the steady state level of Fc gamma RI mRNA by IFN-gamma and dexamethasone in human monocytes, neutrophils, and U-937 cells. *J. Immunol.* **145**:267–275 (1990).

37. P. G. Comber, V. Lentz, and A. D. Schreiber. Modulation of the transcriptional rate of Fc gamma receptor mRNA in human mononuclear phagocytes. *Cell Immunol.* **145**:324–338 (1992).
38. H. Kyle, J. P. Ward, and J. G. Widdicombe. Control of pH of airway surface liquid of the ferret trachea *in vitro*. *J. Appl. Physiol.* **68**:135–140 (1990).
39. D. W. Nielson, J. Goerke, and J. A. Clements. Alveolar subphase pH in the lungs of anesthetized rabbits. *Proc. Natl. Acad. Sci. USA* **78**:7119–7123 (1981).
40. M. Raghavan, Y. Wang, and P. J. Bjorkman. Effects of receptor dimerization on the interaction between the class I major histocompatibility complex-related Fc receptor and IgG. *Proc. Natl. Acad. Sci. USA* **92**:11200–11204 (1995).